remote sensing

MDPI

Article

Improved Ultra-Rapid UT1-UTC Determination and Its Preliminary Impact on GNSS Satellite Ultra-Rapid Orbit Determination

Fei Ye [1], Yunbin Yuan [1,*] and Zhiguo Deng [2]

[1] State Key Laboratory of Geodesy and Earth's Dynamics, Innovation Academy for Precision Measurement Science and Technology, Chinese Academy of Sciences, Wuhan 430077, China; feiye@apm.ac.cn

[2] Deutsches GeoForschungsZentrum, TELEGRAFENBERG 1, Deutschland, 14473 Potsdam, Germany; deng@gfz-potsdam.de

* Correspondence: yybgps@whigg.ac.cn; Tel.: +86-027-6888-1072

Received: 24 August 2020; Accepted: 30 October 2020; Published: 31 October 2020



Abstract: Errors in ultra-rapid UT1-UTC primarily affect the overall rotation of spatial datum expressed by GNSS (Global Navigation Satellite System) satellite ultra-rapid orbit. In terms of existing errors of traditional strategy, e.g., piecewise linear functions, for ultra-rapid UT1-UTC determination, and the requirement to improve the accuracy and consistency of ultra-rapid UT1-UTC, the potential to improve the performance of ultra-rapid UT1-UTC determination based on an LS (Least Square) + AR (Autoregressive) combination model is explored. In this contribution, based on the LS+AR combination model and by making joint post-processing/rapid UT1-UTC observation data, we propose a new strategy for ultra-rapid UT1-UTC determination. The performance of the new strategy is subsequently evaluated using data provided by IGS (International GNSS Services), iGMAS (international GNSS Monitoring and Assessment System), and IERS (International Earth Rotation and Reference Systems Service). Compared to the traditional strategy, the numerical results over more than 1 month show that the new strategy improved ultra-rapid UT1-UTC determination by 29–43%. The new strategy can provide a reference for GNSS data processing to improve the performance of ultra-rapid products.

Keywords: GNSS; ultra-rapid UT1-UTC determination; LS + AR; piecewise linear function; ultra-rapid orbit determination

1. Introduction

In recent years, the requirement of GNSS (Global Navigation Satellite System) to have real-time precise positioning is becoming more and more urgent for real-time detection research in the field of Earth sciences and for the increasing number of real-time high-precision positioning applications [1–3]. GNSS satellite ultra-rapid orbit is the key in determining real-time precise orbits and achieving real-time precision point positioning (PPP) [4,5]. The accuracy and stability of GNSS satellite ultra-rapid orbit determination directly or indirectly affects and limits the performance and promotion of real-time PPP and related applications [6–8]. UT1 is the angle of the Earth's rotation about the CIP (Celestial Intermediate Pole) axis defined by its conventional linear relation to the Earth Rotation Angle (ERA), and UT1-UTC is the difference between the UT1 parameter derived from observations and UTC (Coordinated Universal Time) [9]. Ultra-rapid UT1-UTC is currently one of the main factors affecting the performance of GNSS satellite ultra-rapid orbit determination [10]. Compared with the present performance, the existing error in ultra-rapid UT1-UTC has a significant impact on ultra-rapid orbit determination [6,11–13]. Therefore, further improvement in the processing strategy of ultra-rapid

UT1-UTC determination will significantly improve the performance of spatial datum expressed by GNSS satellite ultra-rapid orbit.

In general, the research of UT1-UTC prediction involved in satellite precise orbit determination mainly focuses on the construction and evaluation of UT1-UTC prediction models. The current prediction models can be divided into linear models [12,14], nonlinear models [15], and their improved models [16–20]. Global ERP (Earth rotation parameter) prediction and test results have been compared by the Vienna University of Technology and IERS (International Earth Rotation and Reference Systems Service), and they showed it is impossible to use the current prediction models to accurately predict ERP under various conditions [21,22]. Compared to other models such as spectral analysis, kalman filter, and neural networks, the LS (Least Square) + AR (Autoregressive) combination model has a good performance for short-term prediction of UT1-UTC based on C04 provided by IERS [21,23]. The UT1-UTC prediction sequence provided by IERS is generally generated directly by these models or their combined models [24,25]. Because this prediction sequence cannot directly apply to GNSS satellite ultra-rapid orbit solution, it is usually necessary to obtain ultra-rapid UT1-UTC after further processing this sequence [10]. At present, in ultra-rapid orbit determination, a piecewise linear function is generally used to process the consecutive single types of UT1-UTC observation data, e.g., Bulletin A, for several days provided by IERS to obtain the ultra-rapid UT1-UTC. However, Wang et al. [13] has shown that the correlation coefficients for the interpolated UT1-UTC of true values and fitting values are gradually reduced when the time resolution of UT1-UTC is increased, and using only the consecutive single type of UT1-UTC observation data over several days to determine ultra-rapid UT1-UTC may also need to be further analyzed and discussed. On the other hand, there is systematic bias in GNSS-based length-of-day (LOD) with respect to the values of EOP (Earth orientation parameter) 14 CO4 of IERS, and it is possible to improve the effect of this systematic bias and provide a more reliable initial value for ultra-rapid LOD derived from ultra-rapid UT1-UTC [26].

Accordingly, compared to the traditional strategy, e.g., the piecewise linear function, there is potential to further improve the performance of ultra-rapid UT1-UTC when using the joint products released by IERS to generate ultra-rapid UT1-UTC based on the LS+AR combination model. Therefore, the research and analysis of ultra-rapid UT1-UTC determination used for ultra-rapid orbit determination are carried out. We propose a new strategy for ultra-rapid UT1-UTC determination based on joint post-processing/rapid UT1-UTC observation data (EOP 14 C04 and IERS gpsrapid.daily) and an LS+AR combination model. The basic model and strategy are described in detail in the "Materials and Methods" section. Then, the new strategy is evaluated, and the 29–43% performance improvement is displayed. Finally, discussions and summaries are given.

2. Materials and Methods

Preprocessing of UT1-UTC, including removing leap seconds and tides, is firstly performed before applying it to the combination model of LS and AR [27]. TAI (International Atomic Time) can be obtained after removing leap seconds from UTC, and UT1R can be obtained after tidal effects are removed from UT1. The UT1R-TAI time series obtained after preprocessing can all be divided into three parts: periodic, linear, and residual terms. The periodic and linear terms can be fitted and extrapolated by the LS model, and the residual terms can be fitted by the LS model and predicted by the AR model [14,28]. A brief principle of the combined LS + AR model and a new strategy for ultra-rapid UT1-UTC determination are introduced in the following.

2.1. Basic Principles of LS + AR Combination Model

The fitted equation of an LS model for periodic and linear terms of UT1R-TAI can be written as follows [29]:

$$f_t = a + bt + \sum_{i=1}^{k} [c_i \cos(2\pi t/PE_i) + d_i \sin(2\pi t/PE_i)] \quad (1)$$

where f_t is the time sequence of UT1R-TAI; k refers to the number of periodic terms in these series; PE_i is the corresponding oscillation period obtained by spectrum analysis; and a, b, c_i, and d_i are the unknown parameters to be estimated.

The equation of the $AR(p)$ model for the fitted residual terms of UT1R-TAI can be written as follows [29,30]:

$$Z_t = \sum_{i=1}^{p} \varphi_i Z_{t-i} + a_t \tag{2}$$

where φ_i is the unknown parameter to be estimated, Z_t is the fitted residual terms, a_t refers to white noise, p is the order of the AR model, and the search range of p is $1 \sim \sqrt{N}$; the rule for estimating the AR model order is to take the minimum values of FPE (Final Prediction Error) [31], AIC (Akaike Information Criterion) [32], and BIC (Bayes Information Criterion) [33], where N represents the number of residual terms used for modeling.

In evaluating the quality of earth rotation parameters, the mean absolute error (MAS) [27] adopted by EOP PCC (prediction comparison campaign) can be written as follows:

$$(MAE)_l = \frac{1}{N}\sum_{i=1}^{N}\left|O_i^l - P_i^l\right| \tag{3}$$

where l and N are the prediction span and the number of prediction periods, respectively. O_i^l and P_i^l refer to the reference value and predicted value of earth rotation parameters. The value of $\left|O_i^l - P_i^l\right|$ is the absolute residual.

2.2. New Strategy of Ultra-Rapid UT1-UTC Determination for Ultra-Rapid Orbit

Figure 1 shows the new strategy for ultra-rapid UT1-UTC determination based on the LS + AR combination model and the traditional strategy. The other details for new strategy are displayed in the following.

Ultra-rapid UT1-UTC includes observation and prediction parts, and a description of the UT1-UTC observation data used by our new strategy for different periods is summarized in Figure 2. Among them, the green line and red line represent the observation and prediction parts of the ultra-rapid ERP, respectively. In fact, UT1-UTC can only be determined from the VLBI (Very Long Baseline Interferometry) technique and derived from Lunar Laser Ranging (LLR) in a limited scope [34]. Different from other parameters in ultra-rapid ERP, Figure 2 also shows that UT1-UTC cannot be solved directly by GNSS [35] and that the observation part in ultra-rapid UT1-UTC should also be predicted. In Figure 2, 00, 06, 12, and 18 represent time periods of four ultra-rapid products per day. In addition, Figures 1 and 2 show the general idea of the new strategy for ultra-rapid UT1-UTC determination, which includes joint UT1-UTC data in Figure 1 that comes from EOP 14 C04 and IERS gpsrapid.daily.

Based on the joint UT1-UTC data sequence and time delay of the observed UT1-UTC data, in order to determine ultra-rapid UT1-UTC, at least 2 days of UT1-UTC need to be predicted (Figure 2); thus, two processing methods are designed to determinate ultra-rapid UT1-UTC:

Method 1 (A)—The UT1-UTC data sequence is predicted for 2 days, and then the second-order Lagrange interpolation algorithm is used to obtain the observation and prediction parts of the ultra-rapid UT1-UTC parameter, which is updated once a day.

Method 2 (B)—The UT1-UTC data sequence is predicted for one day, and then the predicted value of this step is added to the original sequence again for a 1-day prediction. Finally, the second-order Lagrange interpolation algorithm is used to obtain the observation and prediction parts of the ultra-rapid UT1-UTC parameter, which is updated once a day.

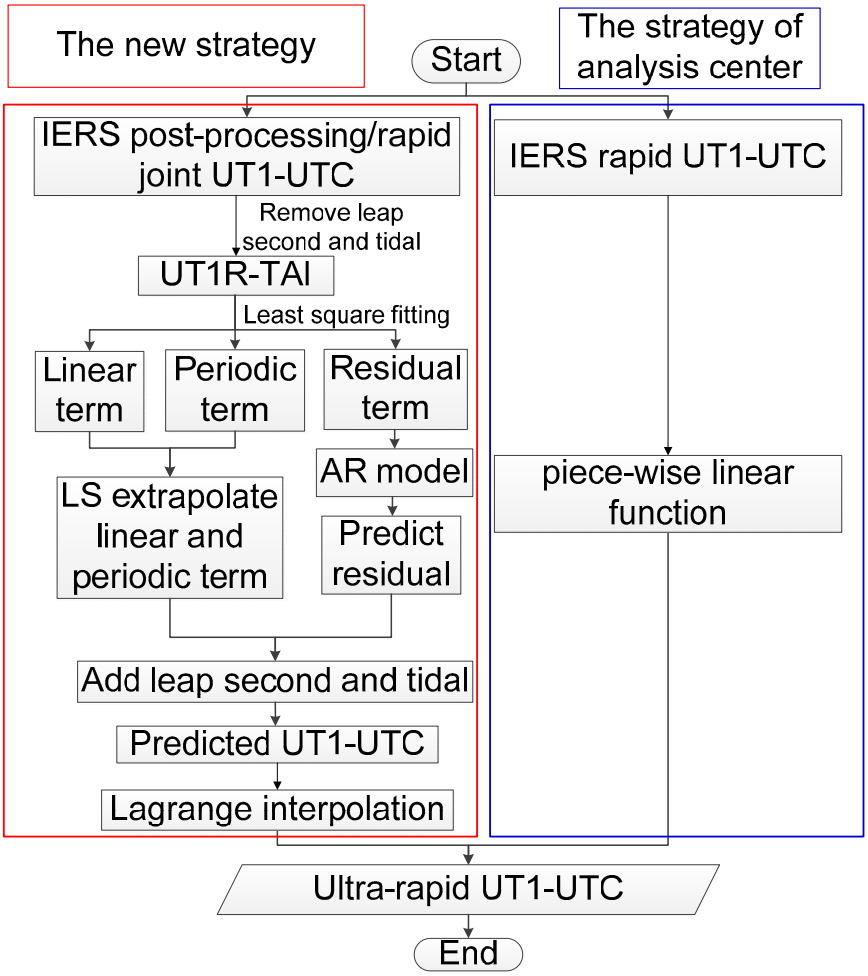


Figure 1. Strategies for ultra-rapid UT1-UTC determination. The periodic, linear, and residual terms of UT1R-TAI (**left**) extracted from UT1-UTC are fitted by LS. The periodic and linear terms of UT1R-TAI (**left**) are extrapolated, and the residual terms are predicted. The strategy of analysis center (**right**) is the traditional strategy for ultra-rapid UT1-UTC determination.

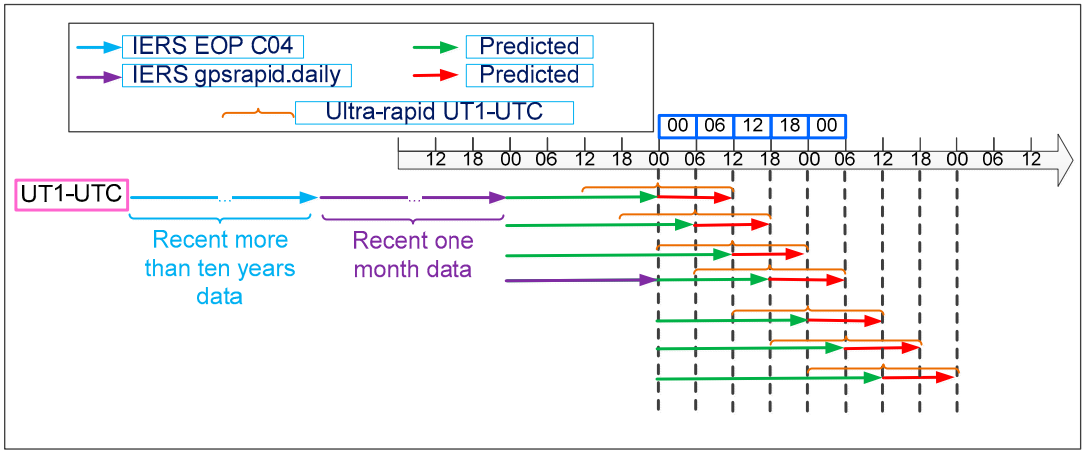


Figure 2. Summary of the UT1-UTC observation data used for ultra-rapid UT1-UTC determination by the new strategy. The observation data used for ultra-rapid UT1-UTC determination are from EOP 14 C04 and IERS gpsrapid.daily.

For Method 1 (A), the prediction span is directly 2 days. For Method 2 (B), iterative prediction is adopted, where each prediction span is one day. Compared to Method 1 (A), each prediction span in

Method 2 (B) is smaller, but the final observed UT1-UTC data in the second iteration are simulated, whereas the UT1-UTC data in Method 1 (A) are all observed. Therefore, the performance of the two methods should be evaluated by experimentation and analysis, and the best processing method will be considered in the new strategy.

3. Results

The quality of ultra-rapid UT1-UTC based on different cases was firstly analyzed in detail. In this experiment, data from EOP 14 C04, IERS gpsrapid.daily, and IGS (International GNSS Services) and iGMAS (international GNSS Monitoring and Assessment System) ultra-rapid products were used. Here, MJD (Modified Julian Date) 58356–58400 was the test period, and when calculating MAS, the reference values were from EOP 14 C04 and determined (predicted) values, including observation and prediction parts from different cases. The initial MJDs were 54,466 (EOP 14 C04), 58,326 (IERS gpsrapid.daily), and 58,326 (ultra-rapid products).

To analyze and compare the performance of new and traditional strategies, four cases [Case 1 (A), Case 2 (B), Case 3 (iGMAS), and Case 4 (IGU)] were conducted. In this part, ultra-rapid UT1-UTC for different cases was first obtained, and then the absolute residuals and MAS of different cases were subsequently calculated by comparing these ultra-rapid UT1-UTCs with EOP 14 C04.

Cases 1 (A) and 2 (B) are designed to analyze the performance of Methods 1 (A) and 2 (B) in the new strategy. Cases 3 (iGMAS) and 4 (IGU) are designed to analyze performance related to the traditional strategy. Here, Case 1 (A) is where the ultra-rapid UT1-UTC parameter is generated by Method 1 (A), and Case 2 (B) is where the ultra-rapid UT1-UTC parameter is generated by Method 2 (B). Both Cases 1 (A) and 2 (B) generate ultra-rapid UT1-UTC based on more than 10-year joint products and the LS+AR combination model. Additionally, Case 3 (iGMAS) is where the ultra-rapid UT1-UTC parameter is provided by iGMAS ultra-rapid products, and Case 4 (IGU) is where the ultra-rapid UT1-UTC parameter is provided by IGS ultra-rapid products. Both iGMAS ultra-rapid and IGS ultra-rapid products generate ultra-rapid UT1-UTC based on piecewise linear functions and consecutive rapid UT1-UTC observation data for several days.

Figure 3 shows the results determined for ultra-rapid UT1-UTC for different cases, in which the top panel of Figure 3 shows the absolute residuals of the observed part under different processed cases, and the bottom panel of Figure 3 is the absolute residuals of the predicted part. The legends in Figure 3 are the mean absolute errors of UT1-UTC parameters for observed and predicted parts in the ultra-rapid product. The residual distributions for Cases 2 (B) and 4 (IGU) are also displayed in Appendix A. Table 1 presents the summary of Figure 3 as well as the relative gain (RG) of ultra-rapid UT1-UTC for case 2 compared to IGS and iGMAS ultra-rapid products.

Table 1. Relative gain of ultra-rapid UT1-UTC determination for case 2 (B) compared to IGS and iGMAS ultra-rapid products.

Parameter	Cases	MAE (μs)		Relative Gain (%)	
				IGU	iGMAS
Ultra-rapid UT1-UTC	B	Observed part	51	42.70	42.05
		Predicted part	68	29.17	37.61
	IGU	Observed part	89	-	-
		Predicted part	96	-	-
	iGMAS	Observed part	88	1.12	-
		Predicted part	109	−13.54	-

In the above, $(\textbf{relative gain})_T = 100 \times (\mathrm{MAE1} - \mathrm{MAE2})/\mathrm{MAE1}$; MAE2 and MAE1 are the MAEs of Case B (or iGMAS) and IGU when T represents IGU; similarly, MAE2 and MAE1 are the MAEs of Case B and iGMAS when T represents iGMAS.

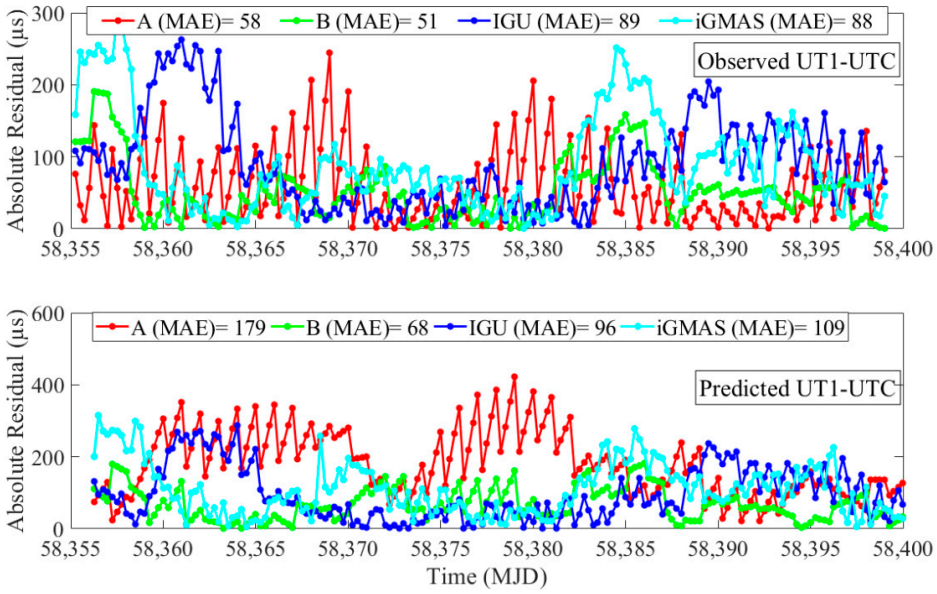


Figure 3. Results of observed (**top**) and predicted (**bottom**) parts in ultra-rapid UT1-UTC determination.

Compared to other cases, either observed UT1-UTC or predicted UT1-UTC, Figure 3 and Appendix A show that case 2 (B) had the best performance. This indicates that the prediction span seriously impacts the prediction performance of ultra-rapid UT1-UTC. After shortening the prediction span, the performance of iterative predictions was better. In addition, from Table 1, compared to Case 4 (IGU), we can see that case 2 (B) improved by 42.70% and 29.17% for the observed and predicted parts, respectively. At the same time, compared to Case 3 (iGMAS), case 2 (B) improved by 42.05% and 37.61%. From the above results, it was concluded that the new strategy for ultra-rapid UT1-UTC determination should follow Method 2 (B).

4. Discussion

The above results show that using the joint products and LS+AR combination model improved the accuracy and consistency of ultra-rapid UT1-UTC determination and IERS EOP 14 C04. In order to analyze and discuss the direct and extended applications of this new strategy, the preliminary impact on ultra-rapid orbit determination is firstly assessed. In addition, the preliminary prediction and quality assessment of ultra-rapid LOD is performed.

4.1. Discussion of Ultra-Rapid Orbit Determination

This section only assesses the coordinate transformation impact of ultra-rapid UT1-UTC on orbits coordinate of prediction part in the ultra-rapid product. The experimental steps designed to analyze the impact of using ultra-rapid UT1-UTC in transforming coordinates from the celestial reference frame (defined by the mean pole and equinox at J2000.0) to the terrestrial frame (IGS14) are as follows:

(1) Obtain the simulated true satellite orbit state—the initial state of satellite orbit and the related state transition matrix are fitted by the final precise orbit and ERP products.
(2) Obtain the simulated true satellite orbit coordinates in J2000.0—the coordinates of the satellite in ultra-rapid orbit in the celestial reference frame are calculated by integrating the satellite state parameters and related state transition matrix obtained in the first step and the final precise ERP products.
(3) Obtain the satellite orbit coordinates in IGS14 with different ultra-rapid ERPs [36]—the coordinates of the satellite in ultra-rapid orbit obtained in the second step and the ultra-rapid ERPs (IGG ERP and IGU ERP, where IGG ERP represents ultra-rapid UT1-UTC and is generated by the above new strategy; other parameters in ultra-rapid ERP come from the IGS ultra-rapid product, and IGU

ERP represents ultra-rapid ERP and is provided by the IGS ultra-rapid product) obtained in the above part are used to transform the coordinates of the satellite in ultra-rapid orbit in the terrestrial frame.

(4) Comparative analysis—the 6-hour prediction for each arc of satellite in ultra-rapid orbit obtained in the third step is compared with the final precise orbit products, and the residual of each satellite and its maximum (Max), average (Ave), and RMS (Root Mean Square) are calculated.

The experimental period was MJD 58356–58400, and the final precise orbit and ERP products are provided by IGS. Figure 4 represents the coordinate residuals between the 6-hour prediction of ultra-rapid orbits and the IGS final precise orbits in the X, Y and Z directions when IGG ERP is used. Similarly, Figure 5 represents these coordinate residuals when IGU ERP is used.

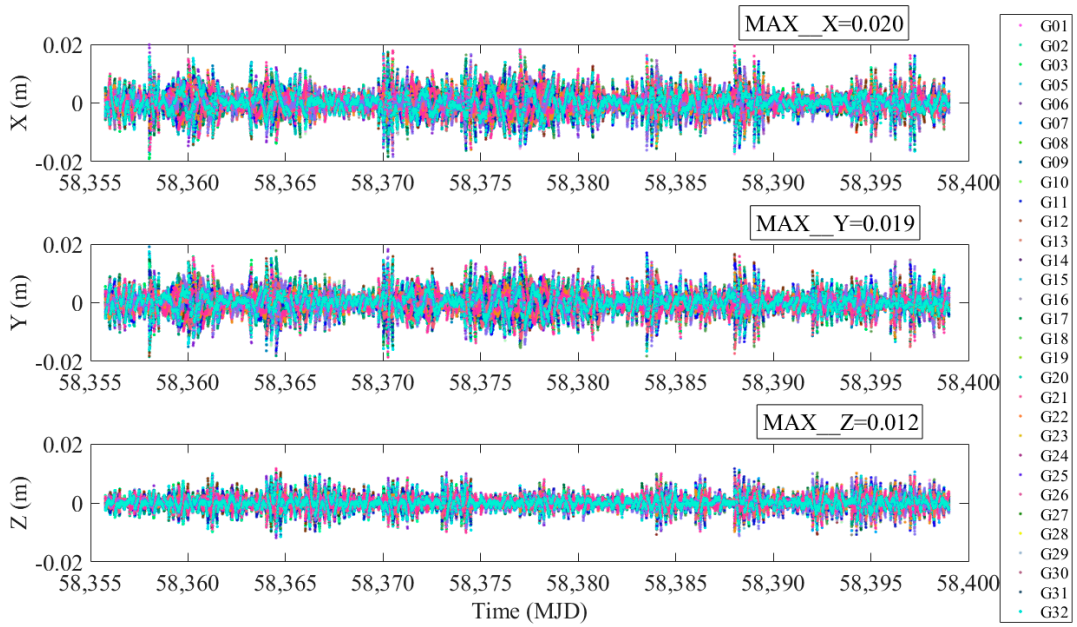


Figure 4. Coordinate residuals between the 6-hour predicted part of ultra-rapid orbits and the IGS final precise orbits in the X, Y, and Z directions when IGG ERP is used. MAX_X, MAX_Y, and MAX_Z are the maximum residuals for all satellites in X, Y, and Z directions, respectively.

Figure 4 shows that the maximum residuals for all satellites are 2.0 and 1.9 cm in the X and Y directions when IGG ERP is used. Figure 5 shows the maximum residuals are 2.4 and 2.5 cm when IGU ERP is used. Therefore, compared to the maximum residuals for all satellites when IGU ERP is used, the maximum residuals on coordinate transformation in ultra-rapid orbit determination are improved by 17% and 24% in the X and Y directions, respectively, when IGG ERP is used. Both Figures 4 and 5 show that the maximum residuals for all satellites are 1.2 cm. The error in the Z direction is caused by polar motion; polar motion is not the subject of our discussion here, so only the X and Y directions are displayed when the maximum, average, and RMS of residuals of each satellite are calculated in next analysis.

The top panel in Figure 6 represents the residual statistics of the 6-hour prediction for each arc for all satellites in the X and Y directions, respectively. The bottom panel in Figure 6 represents the improved percentages of residual statistics for all satellites in the X and Y directions, respectively. Figure 6 shows that the residuals when IGG ERP is used are better than the residuals when IGU ERP is used, in terms of maximum and average residuals. However, the expected improvement in the RMS of residuals was not seen, and this phenomenon may be due to the better consistency of UT1-UTC parameters between the final and ultra-rapid ERP products provided by IGS. Therefore, the UT1-UTC residuals and statistics between the final ERP products provided by IGS and EOP 14 C04 provided by IERS are also calculated here, as shown in Figure 7. From Figure 7, it can be seen that the UT1-UTC

parameter sequence provided by IGS in the final ERP products had a deviation of about 63.15 μs from the UT1-UTC parameter sequence published by IERS in EOP 14 C04. On the other hand, in terms of the absolute RMS and the accuracy of ultra-rapid orbits, the RMS of residuals can be considered equivalent when IGG ERP and IGU ERP are used.

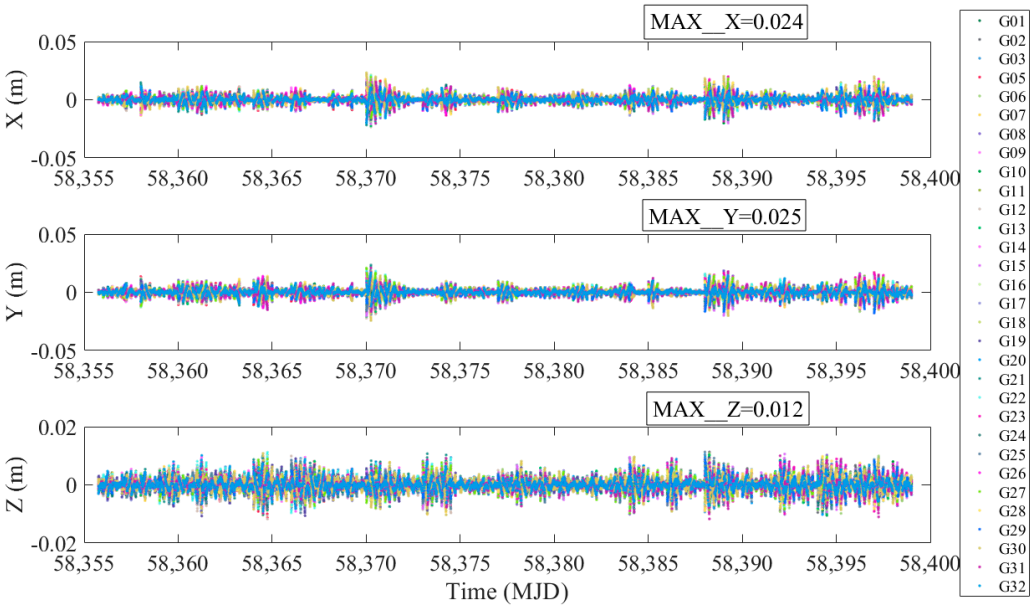


Figure 5. Coordinate residuals between the 6-hour predicted part of ultra-rapid orbits and the IGS final precise orbits in the X, Y, and Z directions when IGU ERP is used. MAX_X, MAX_Y, and MAX_Z are the maximum residuals for all satellites in X, Y, and Z directions, respectively.

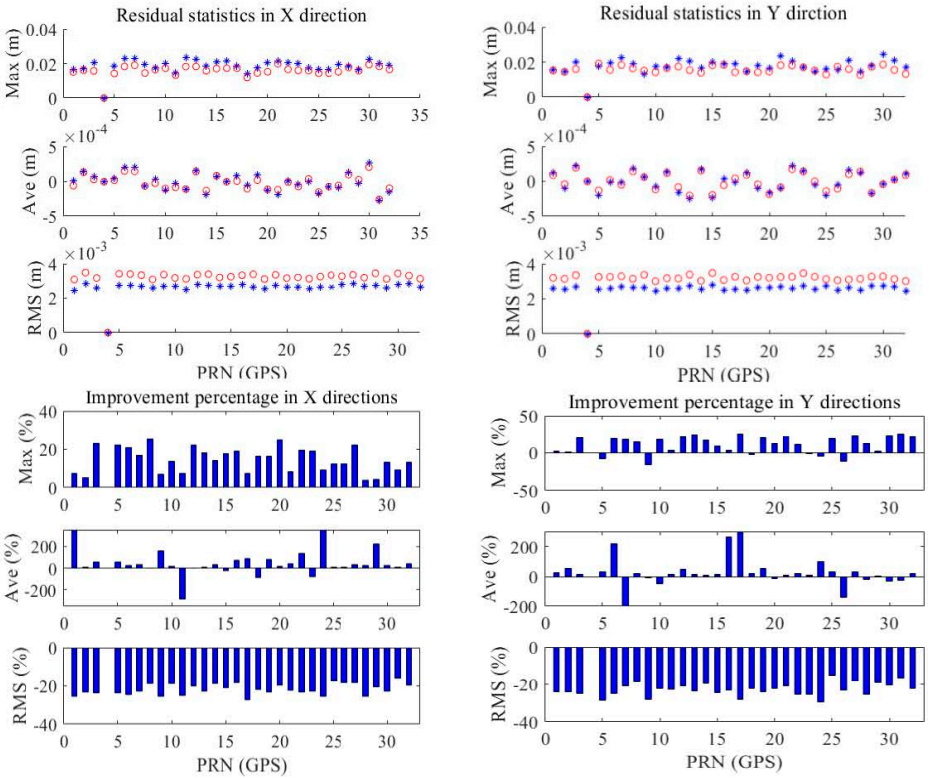


Figure 6. The residual statistics and the improved percentages for all satellites in the X and Y directions (in the top panel, blue represents IGG, while red represents IGU ERP).

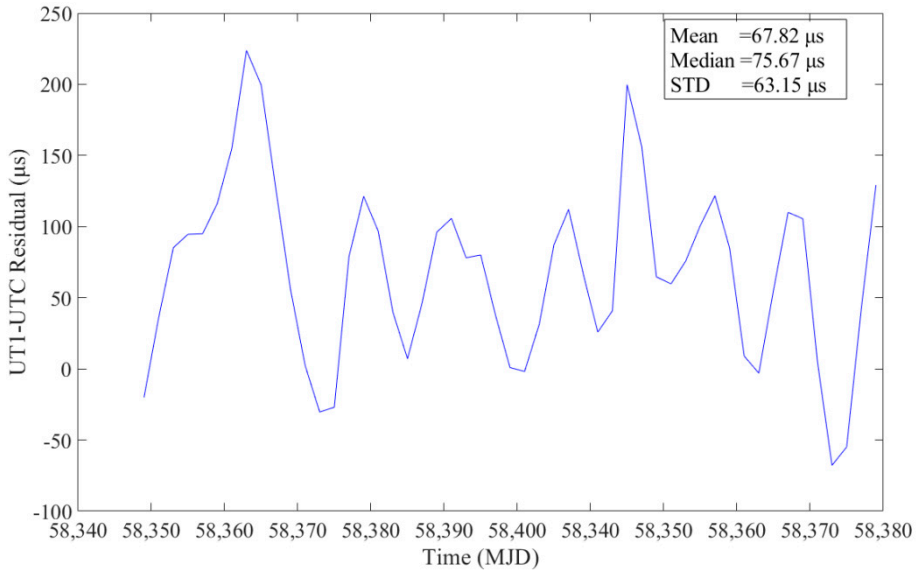


Figure 7. UT1-UTC residuals and statistics between the IGS final precise ERPs and the IERS EOP 14 C04.

4.2. Discussion on Ultra-Rapid LOD Determination

Ultra-rapid LOD includes observation and prediction parts, and a description of LOD observation data used by the new strategy for ultra-rapid LOD prediction in different periods is summarized in Figure 8.

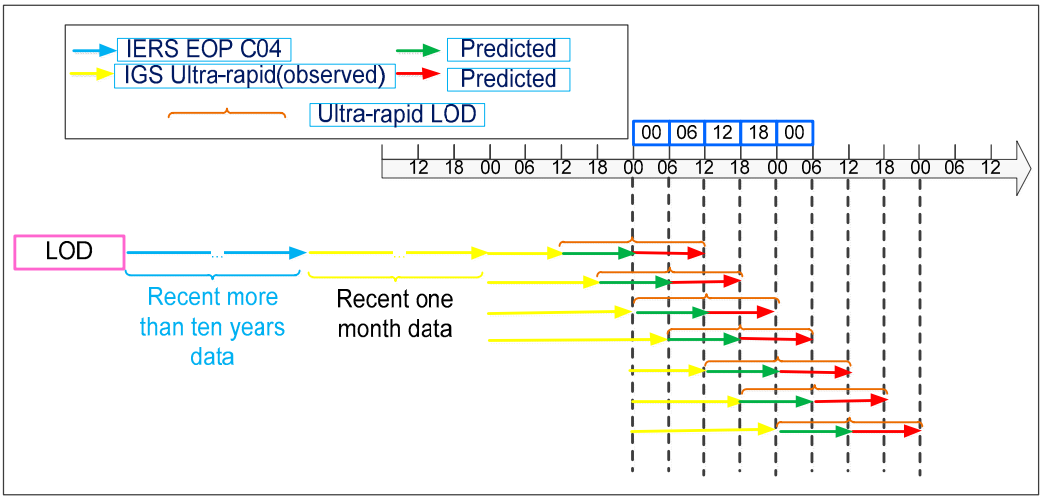


Figure 8. Summary of the LOD observation data used for ultra-rapid LOD prediction by the new strategy. The observation data used for ultra-rapid LOD prediction are from EOP 14 C04 and observation part of IGS ultra-rapid products.

Different from ultra-rapid UT1-UTC determination, Figure 8 shows that the observation part in ultra-rapid LOD can be solved directly by GNSS, and only the prediction part should be predicted. Therefore, two processing methods are designed to obtain the prediction part in ultra-rapid LOD as follows:

Method 1 (A)—LOD data sequences are predicted for one day, which is updated every 6 h.

Method 2 (B)—LOD data sequences are resampled by a second-order Lagrange interpolation algorithm, and then the data sequences after resampling are predicted for 1 day and updated every 6 h.

The data from EOP 14 C04 [MJD: 54,466–58,400 and MJD: 58,356–38,400 are the test period as the reference (true) value compared to the determined value, also namely prediction part value, of different cases], and IGS and iGMAS ultra-rapid products (MJD: 58,326–58,400) are used, and four cases [Case 1 (A), Case 2 (B), Case 3 (iGMAS), and Case 4 (IGU)] are conducted similarly.

Figure 9 shows the absolute residuals of the LOD parameter for predicted parts under different processed cases, and the legend in Figure 9 shows mean absolute errors of the LOD parameter for predicted parts in the ultra-rapid product. Table 2 presents a summary of Figure 9 and the relative gain of the LOD parameter for the predicted part in case 1 compared to IGS and iGMAS products. From Table 2, compared to Case 4 (IGU), we can see that the improvement in case 1 (A) was 20.83%. At the same time, compared to Case 3 (iGMAS), the improvement in case 1 (A) was 64.81%.

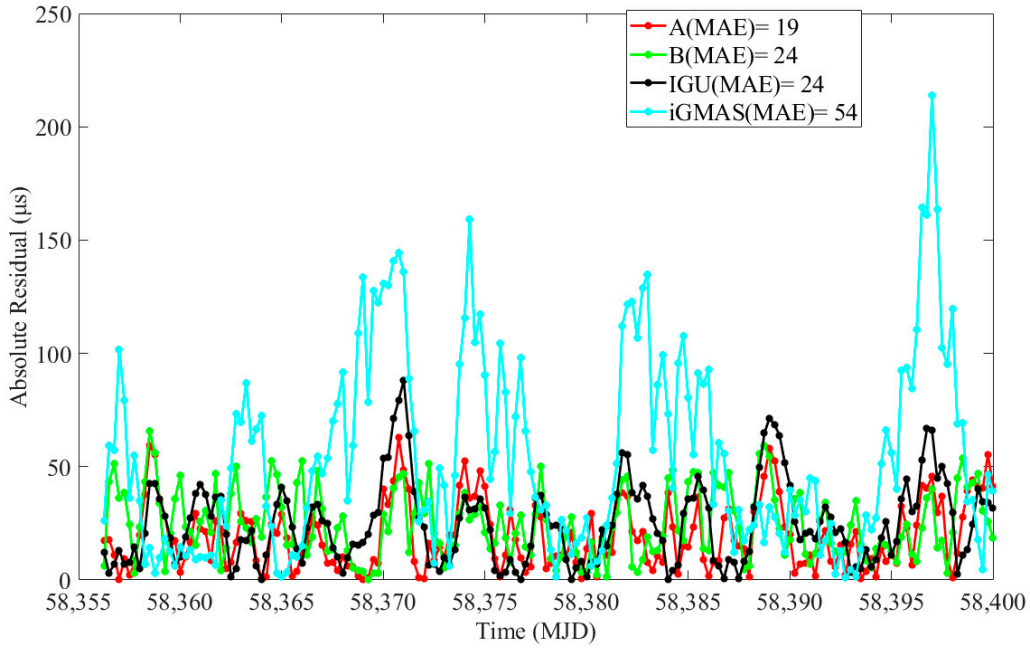


Figure 9. Results of the prediction part of ultra-rapid LOD.

Table 2. Relative gain of predicted LOD for case 1 (A) compared to IGS and iGMAS products.

Parameter	Strategies	MAE (μs)	Relative Gain (%)	
			IGU	iGMAS
the prediction part of ultra-rapid LOD	A	19	20.83	64.81
	IGU	24	-	-
	iGMAS	54	−125.00	-

In the above, $(\textbf{relative gain})_T = 100 \times (\text{MAE1} - \text{MAE2})/\text{MAE1}$; MAE2 and MAE1 are the MAEs of Case A (or iGMAS) and IGU when T represents IGU; similarly, MAE2 and MAE1 are the MAEs of Case A and iGMAS when T represents iGMAS.

Therefore, based on the LS + AR combination model, the above assessment shows that the new strategy further improves the performance of ultra-rapid UT1-UTC determination and the prediction performance of ultra-rapid LOD when using joint observation data.

On the one hand, ultra-rapid UT1-UTC determined by the new strategy can directly apply to GNSS satellite ultra-rapid orbit determination and can directly constrain the known value. The prior value in ultra-rapid LOD can also be derived directly from ultra-rapid UT1-UTC. In addition, ultra-rapid LOD prediction directly by the new strategy should depend on the observation part in ultra-rapid LOD, so iterations are essential, and the time consumed needs to be balanced. Therefore, the impact of the new strategy for ultra-rapid LOD on ultra-rapid orbit determination needs to be further analyzed and researched. In addition, typically a combination of GNSS [37] and Satellite Laser Ranging (SLR)

observations in the LAser GEOdynamics Satellite (LAGEOS) and Etalon satellites are used to determine LOD [38]. In a limited scope, Doppler Orbitography and Radio-positioning Integrated by Satellite (DORIS) observations can be employed to derive LOD values as well [39]. These observations will be used to enrich the strategy in the future.

On the other hand, it is worth noting that EOP 14 C04 and IERS gpsrapid.daily sometimes have increased latency in practice, which will result in a slower performance of the new strategy. However, as long as the two products are released on time, the performance will be ensured Compared to the LS+AR combination model, the other improved prediction models and methods (e.g., [16,17]) can also be used in this new strategy after appropriate modifications, and the performance should be better. However, this was not assessed and verified here, and future works are required.

5. Conclusions

In order to explore the potential to improve the accuracy and consistency of ultra-rapid UT1-UTC determination to better serve ultra-rapid orbit determination of GNSS satellites, this study has proposed a new strategy related to ultra-rapid UT1-UTC. Furthermore, to assess the performance of the new strategy, we used UT1-UTC data of EOP 14 C04 provided by IERS, daily rapid products provided by IERS, and ultra-rapid products provided by IGS and iGMAS.

The ultra-rapid UT1-UTC test results of the new strategy showed an overall better performance than the ultra-rapid UT1-UTC test results with the traditional strategy. Compared to the UT1-UTC parameter of IGS ultra-rapid products, the improvements to observation and prediction part accuracies were 42.70% and 29.17%, respectively, while compared to the UT1-UTC parameter of iGMAS ultra-rapid products, the improvements were 42.05% and 37.61%, respectively. Results show that the new strategy can improve the maximum and average of residuals for ultra-rapid orbit determination, but the RMS of residuals are almost equivalent. Additionally, the extended application results show that the new strategy can improve the prior value in ultra-rapid LOD.

Different from the traditional strategy, if the complexity of the new strategy is tolerated during ultra-rapid orbit determination, this strategy can provide an available reference to improve the performance of the ultra-rapid UT1-UTC determination and reduce the impact on coordinate transformation between the celestial (inertial) reference frame and the terrestrial frame in ultra-rapid orbit determination.

Author Contributions: F.Y. provided the initial idea for this study; F.Y. and Y.Y. conceived and designed the experiment; F.Y., Y.Y. and Z.D. analyzed the results; F.Y., Y.Y. and Z.D. wrote the paper. All authors have read and agreed to the published version of the final manuscript.

Funding: This work was supported by the Collaborative Precision Positioning Project funded by the Ministry of Science and Technology of China (No. 2016YFB0501900), China Natural Science Funds (No. 42004016) and HuBei Natural Science Funds (No. 2020CFB329).

Acknowledgments: The authors would like to acknowledge the International Earth Rotation and Reference Systems Service (IERS), Multi-GNSS Experiment (MGEX), the Crustal Dynamics Data Information System (CDDIS) of the International GNSS Services (IGS), and Chinese iGMAS networks for providing the data and products. In addition, we also thank these websites (http://www.igs.org/products; http://www.igmas.org/Product; ftp://ftp.igs.org/pub/center/analysis/).

Conflicts of Interest: The authors declare no conflict of interest.

Appendix A

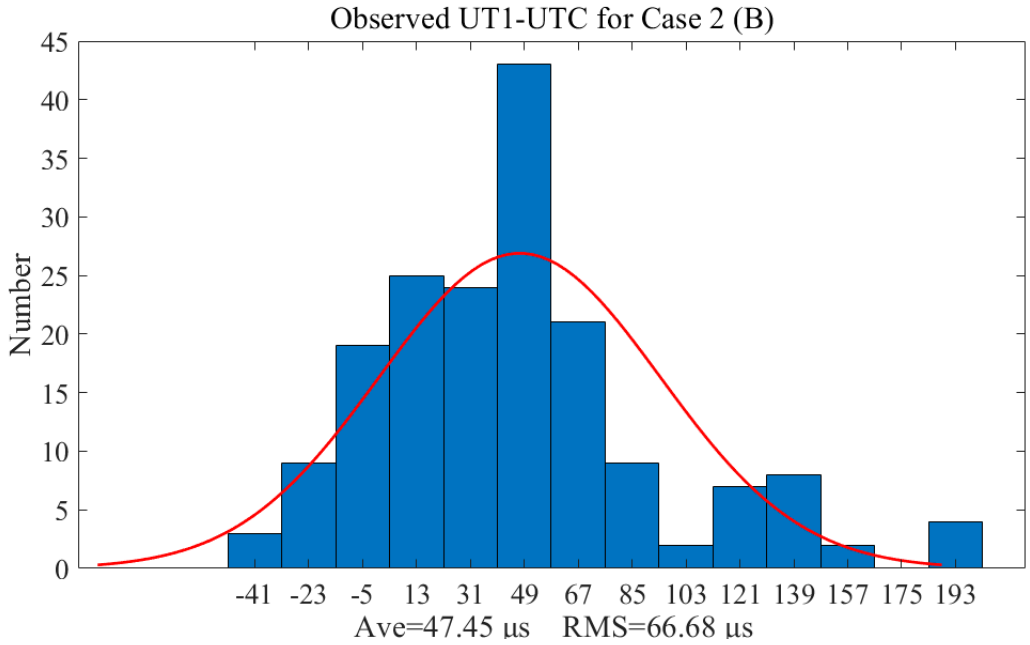


Figure A1. Observation part residual distributions of ultra-rapid UT1-UTC for Case 2 (B).

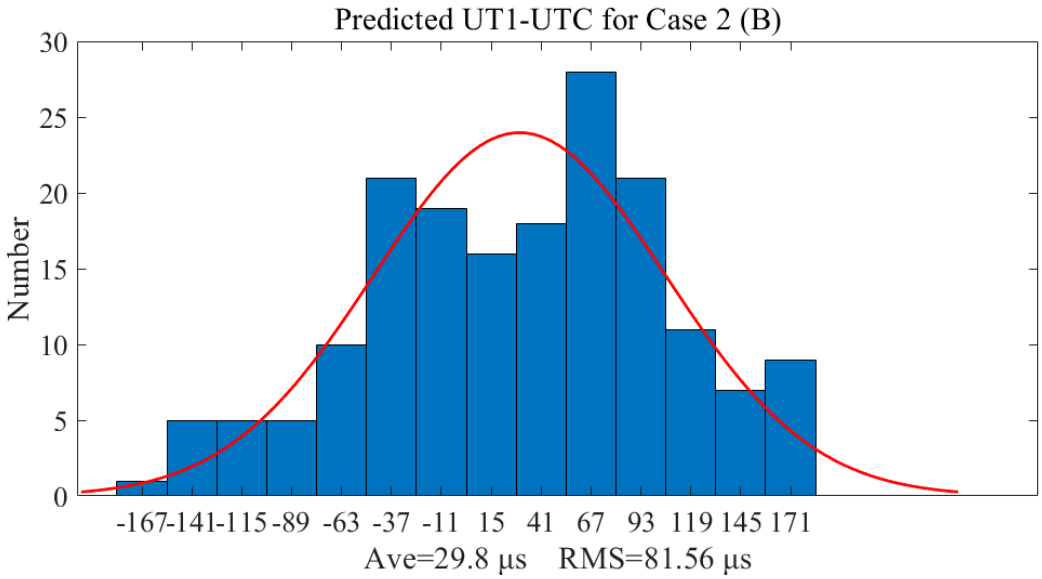


Figure A2. Prediction part residual distributions of ultra-rapid UT1-UTC for Case 2 (B).

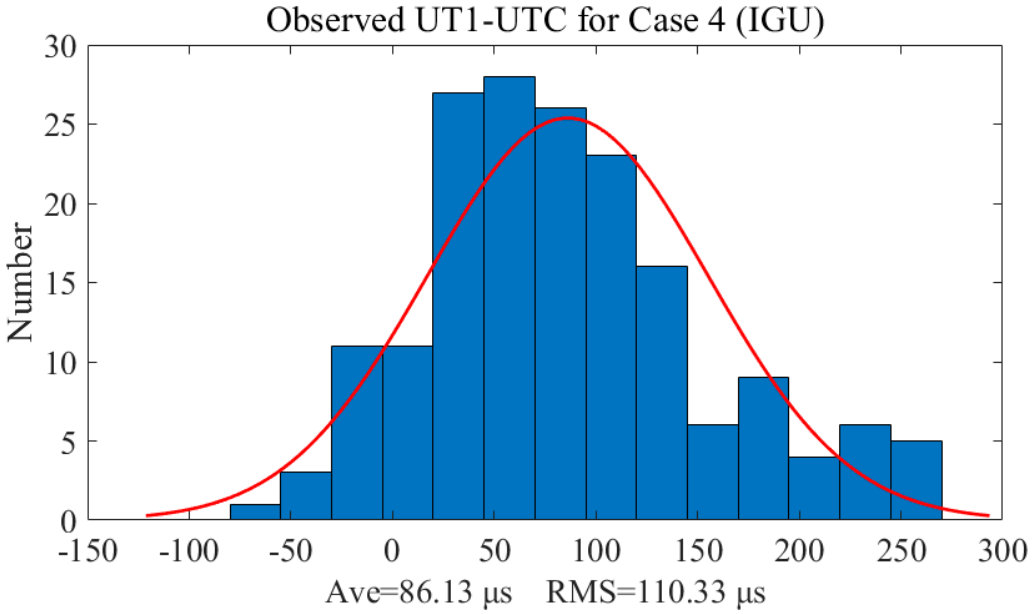


Figure A3. Observation part residual distributions of ultra-rapid UT1-UTC for Case 4 (IGU).

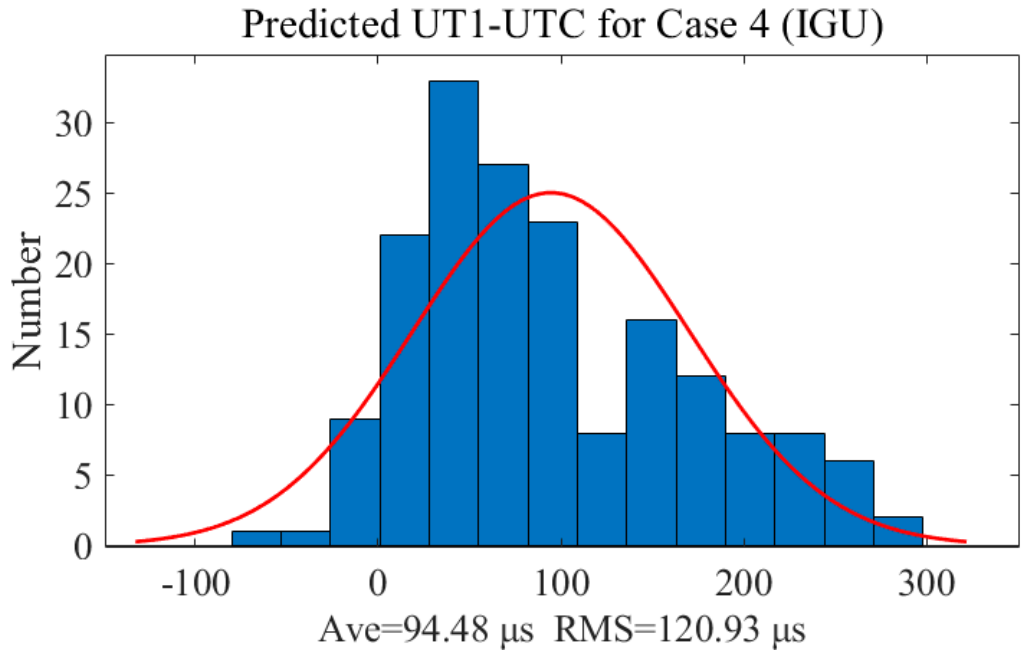


Figure A4. Prediction part residual distributions of ultra-rapid UT1-UTC for Case 4 (IGU).

References

1. Dai, Z.; Zhao, Q.; Lv, Y.; Song, J.; Zhou, J.; Yang, S.; Gu, M. The Wide- and Local-Area Combined GNSS Real-Time Precise Positioning Service System and Products. In Proceedings of the China Satellite Navigation Conference (CSNC) 2017, Shanghai, China, 23–25 May 2017; Volume 3, pp. 409–428.
2. Hu, J.; Zhang, X.; Li, P.; Ma, F.; Pan, L. Multi-GNSS fractional cycle bias products generation for GNSS ambiguity-fixed PPP at Wuhan University. *GPS Solut.* **2019**, *24*, 15. [CrossRef]
3. Jin, S.; Su, K. PPP models and performances from single- to quad-frequency BDS observations. *Satell. Navig.* **2020**, *1*, 16. [CrossRef]
4. Li, X.; Chen, X.; Ge, M.; Schuh, H. Improving multi-GNSS ultra-rapid orbit determination for real-time precise point positioning. *J. Geod.* **2019**, *93*, 45–64. [CrossRef]

5. Ye, F.; Yuan, Y.; Tan, B.; Deng, Z.; Ou, J. The Preliminary Results for Five-System Ultra-Rapid Precise Orbit Determination of the One-Step Method Based on the Double-Difference Observation Model. *Remote Sens.* **2018**, *11*, 46. [CrossRef]
6. Wang, Q.; Zhang, K.; Wu, S.; Zou, Y.; Hu, C. A method for identification of optimal minimum number of multi-GNSS tracking stations for ultra-rapid orbit and ERP determination. *Adv. Space Res.* **2019**, *63*, 2877–2888. [CrossRef]
7. Dousa, J. Development of the GLONASS Ultra-Rapid Orbit Determination at Geodetic Observatory Pecný. In Proceedings of the 2009 IAG Symposium, Buenos Aires, Argentina, 31 August—4 September 2009; pp. 1029–1035.
8. Ye, F.; Yuan, Y.; Zhang, B. Impact analysis of arc length in multi-GNSS ultra-rapid orbit determination based on the one-step method. *Meas. Sci. Technol.* **2020**, *31*, 055012. [CrossRef]
9. Petit, G.; Luzum, B. IERS Conventions. *IERS Tech. Note* **2010**, *36*, 179.
10. Lutz, S.; Beutler, G.; Schaer, S.; Dach, R.; Jäggi, A. CODE's new ultra-rapid orbit and ERP products for the IGS. *GPS Solut.* **2016**, *20*, 239–250. [CrossRef]
11. Wan, L.; Wei, E.; Jin, S. Earth Rotation Parameter Estimation from GNSS and Its Impact on Aircraft Orbit Determination. In Proceedings of the China Satellite Navigation Conference (CSNC) 2014, Nanjing, China, 21–23 May 2014; pp. 105–114.
12. Jia, S.; Xu, T.-H.; Sun, Z.-Z.; Li, J.-J. Middle and long-term prediction of UT1-UTC based on combination of Gray Model and Autoregressive Integrated Moving Average. *Adv. Space Res.* **2017**, *59*, 888–894. [CrossRef]
13. Wang, Q.; Chao, H.; Xu, T.; Chang, G.; Moraleda, A.H. Impacts of Earth rotation parameters on GNSS ultra-rapid orbit prediction: Derivation and real-time correction. *Adv. Space Res.* **2017**, *60*, 2855–2870. [CrossRef]
14. Xu, X.; Zhou, Y. EOP prediction using least square fitting and autoregressive filter over optimized data intervals. *Adv. Space Res.* **2015**, *56*, 2248–2253. [CrossRef]
15. Schuh, H.; Ulrich, M.; Egger, D.; Müller, J.; Schwegmann, W. Prediction of Earth orientation parameters by artificial neural networks. *J. Geod.* **2002**, *76*, 247–258. [CrossRef]
16. Wu, F.; Chang, G.; Deng, K. One-step method for predicting LOD parameters based on LS+AR model. *J. Spat. Sci.* **2019**, 1–12. [CrossRef]
17. Modiri, S.; Belda, S.; Hoseini, M.; Heinkelmann, R.; Ferrándiz, J.M.; Schuh, H. A new hybrid method to improve the ultra-short-term prediction of LOD. *J. Geod.* **2020**, *94*, 23. [CrossRef]
18. Zotov, L.; Xu, X.; Zhou, Y.; Skorobogatov, A. Combined SAI-SHAO prediction of Earth Orientation Parameters since 2012 till 2017. *Geod. Geodyn.* **2018**, *9*, 485–490. [CrossRef]
19. Malkin, Z. Employing Combination Procedures to Short-Time Eop Prediction. *Artif. Satell.* **2010**, *45*, 87–93. [CrossRef]
20. Hu, C.; Wang, Q.; Wang, Z.; Mao, Y. A Method for Improving the Short-Term Prediction Model for ERP Based on Long-Term Observations. In Proceedings of the China Satellite Navigation Conference (CSNC) 2019, Beijing, China, 22–25 May 2019; pp. 24–38.
21. Kalarus, M.; Schuh, H.; Kosek, W.; Akyilmaz, O.; Bizouard, C.; Gambis, D.; Gross, R.; Jovanović, B.; Kumakshev, S.; Kutterer, H.; et al. Achievements of the Earth orientation parameters prediction comparison campaign. *J. Geod.* **2010**, *84*, 587–596. [CrossRef]
22. Shumate, N.A.; Luzum, B.J.; Kosek, W. Earth Orientation Parameters Combination of Prediction Pilot Project. In Proceedings of the Agu Fall Meeting 2013, San Fransisco, CA, USA, 9–13 December 2013; p. G13A-0928.
23. Kosek, W. Future Improvements in EOP Prediction. In Proceedings of the 2009 IAG Symposium, Buenos Aires, Argentina, 31 August—4 September 2009; pp. 513–520.
24. Johnson, T. *IERS Annual Report 2005*; IERS Rapid Service/Prediction Centre: Washington, DC, USA, 2005; pp. 57–66.
25. Dick, W.R.; Thaller, D. *IERS Annual Report 2018*; IERS Rapid Service/Prediction Centre: Washington, DC, USA, 2020; pp. 102–124.
26. Zajdel, R.; Sośnica, K.; Bury, G.; Dach, R.; Prange, L. System-specific systematic errors in earth rotation parameters derived from GPS, GLONASS, and Galileo. *GPS Solut.* **2020**, *24*, 74. [CrossRef]
27. Niedzielski, T.; Kosek, W. Prediction of UT1–UTC, LOD and AAM χ 3 by combination of least-squares and multivariate stochastic methods. *J. Geod.* **2008**, *82*, 83–92. [CrossRef]

28. Niedzielski, T.; Kosek, W. Prediction Analysis of UT1-UTC Time Series by Combination of the Least-Squares and Multivariate Autoregressive Method. In Proceedings of the VII Hotine-Marussi Symposium on Mathematical Geodesy, Rome, Italy, 6–10 June 2009; pp. 153–157.
29. Xu, X.Q.; Zhou, Y.H.; Liao, X.H. Short-term earth orientation parameters predictions by combination of the least-squares, AR model and Kalman filter. *J. Geodyn.* **2012**, *62*, 83–86. [CrossRef]
30. Box, G.E.; Jenkins, G.M.; Reinsel, G.C.; Ljung, G.M. Time series analysis: Forecasting and control. *J. Oper. Res. Soc.* **2015**, *22*, 199–201.
31. Akaike, H. Fitting autoregressive models for prediction. *Ann. Inst. Stat. Math.* **1969**, *21*, 243–247. [CrossRef]
32. Akaike, H. A new look at the statistical model identification. In *Selected Papers of Hirotugu Akaike*; Springer: Berlin/Heidelberg, Germany, 1974; pp. 215–222.
33. Schwarz, G. Estimating the dimension of a model. *Ann. Stat.* **1978**, *6*, 461–464. [CrossRef]
34. Hofmann, F.; Biskupek, L.; Müller, J. Contributions to reference systems from Lunar Laser Ranging using the IfE analysis model. *J. Geod.* **2018**, *92*, 975–987. [CrossRef]
35. Rothacher, M.; Beutler, G.; Herring, T.A.; Weber, R. Estimation of nutation using the Global Positioning System. *J. Geophys. Res. Solid Earth* **1999**, *104*, 4835. [CrossRef]
36. Bizouard, C.; Lambert, S.; Gattano, C.; Becker, O.; Richard, J.-Y. The IERS EOP 14C04 solution for Earth orientation parameters consistent with ITRF 2014. *J. Geod.* **2019**, *93*, 621–633. [CrossRef]
37. Rebischung, P.; Altamimi, Z.; Ray, J.; Garayt, B. The IGS contribution to ITRF2014. *J. Geod.* **2016**, *90*, 611–630. [CrossRef]
38. Pearlman, M.; Arnold, D.; Davis, M.; Barlier, F.; Biancale, R.; Vasiliev, V.; Ciufolini, I.; Paolozzi, A.; Pavlis, E.C.; Sośnica, K.; et al. Laser geodetic satellites: A high-accuracy scientific tool. *J. Geod.* **2019**, *93*, 2181–2194. [CrossRef]
39. Štěpánek, P.; Hugentobler, U.; Buday, M.; Filler, V. Estimation of the Length of Day (LOD) from DORIS observations. *Adv. Space Res.* **2018**, *62*, 370–382. [CrossRef]

Publisher's Note: MDPI stays neutral with regard to jurisdictional claims in published maps and institutional affiliations.



© 2020 by the authors. Licensee MDPI, Basel, Switzerland. This article is an open access article distributed under the terms and conditions of the Creative Commons Attribution (CC BY) license (http://creativecommons.org/licenses/by/4.0/).